November 1, 2003

Equatorial counterelectrojetsduring substorms

T. Kikuchi
K. Hashimoto
T. I. Kitamura
H. Tachihara
Bela G. Fejer, *Utah State University*

Equatorial counterelectrojets during substorms

T. Kikuchi and K. K. Hashimoto
Communications Research Laboratory, Tokyo, Japan

T.-I. Kitamura and H. Tachihara
Department of Earth and Planetary Sciences, Kyushu University, Fukuoka, Japan

B. Fejer
Center for Atmospheric and Space Sciences, Utah State University, Logan, Utah, USA

Received 28 February 2003; revised 2 September 2003; accepted 10 September 2003; published 22 November 2003.

[1] Equatorial counterelectrojet (CEJ) events are analyzed in association with changes in the interplanetary magnetic field (IMF), polar cap potential (PCP), and electric field measured in the equatorial ionosphere. In one event on 16 July 1995, the equatorial CEJ was observed at the afternoon dip equator during the recovery phase of the substorm when the IMF turned northward. Rapid decreases in the PCP and in the auroral electrojet occurred simultaneously with the equatorial CEJ, suggesting instantaneous equatorward penetration of the rapid decrease in the electric field associated with the region 1 field-aligned currents (R1 FACs) under the condition of a well-developed shielding electric field due to the R2 FACs. In the other event on 8 April 1993, the equatorial CEJ associated with the northward turning of the IMF was directly related to a rapid decrease in the equatorial electric field measured by the Jicamarca incoherent scatter radar as well as to a decrease in the PCP. We confirm the scenario for the substorm-associated equatorial CEJ as caused by the dominant R2 FACs when the R1 FACs decrease abruptly because of the northward turning of the IMF. We also suggest that the *DP* 1 current system is composed of the Hall currents surrounding the R2 FACs and the equatorial CEJ closing with the R2 FACs, which are superposed on the *DP* 2 currents caused by the R1 FACs, being dominant when the IMF turns northward. The coherent occurrence of the electric field in the *F* region with the electric current in the *E* region at the equator is explained by applying the Earth-ionosphere waveguide model of *Kikuchi and Araki* [1979b] as a most promising transmission mechanism. All the conditions for the equatorial CEJ most likely occur during the substorm, but the northward turning of the IMF and the resultant decrease in the PCP play a crucial role under the condition of well-developed R2 FACs. *INDEX TERMS:* 2415 Ionosphere: Equatorial ionosphere; 2409 Ionosphere: Current systems (2708); 2411 Ionosphere: Electric fields (2712); 2407 Ionosphere: Auroral ionosphere (2704); 2431 Ionosphere: Ionosphere/magnetosphere interactions (2736); *KEYWORDS:* equatorial counterelectrojet, substorm, region 1 and 2 field-aligned currents

Citation: Kikuchi, T., K. K. Hashimoto, T.-I. Kitamura, H. Tachihara, and B. Fejer, Equatorial counterelectrojets during substorms, *J. Geophys. Res.*, *108*(A11), 1406, doi:10.1029/2003JA009915, 2003.

1. Introduction

[2] It has been reported that the equatorial counterelectrojet (CEJ), defined as a magnetic field decrease below the nighttime level, can be observed at the dayside dip equator [*Gouin*, 1962; *Hutton and Oyinloye*, 1970]. The quiet time CEJ of a timescale of hours has been explained as being caused by the ionospheric dynamo due to atmospheric tidal motions [*Rastogi*, 1974; *Somayajulu et al.*, 1993]. *Fejer et al.* [1976] on the other hand, indicated that the electric field was often reversed in direction, as observed by the Jicamarca incoherent scatter radar during the day and night under quiet and disturbed conditions. They pointed out a possible relation between short-term CEJ and high-latitude electric field variations during disturbed periods.

[3] Magnetic disturbances at the dayside dip equator are often caused by direct penetration of the convection electric field and correlated with disturbances at high latitudes [*Nishida et al.*, 1966; *Onwumechilli et al.*, 1973; *Kikuchi et al.*, 1996, 2000a]. The convection electric field is transmitted from the magnetosphere to the ionosphere accompanying the region 1 field-aligned currents (R1 FACs) [*Iijima and Potemra*, 1976; *Iijima*, 2000]. Ground magnetic signatures of the convection electric field were identified as the quasiperiodic *DP* 2 magnetic fluctuations at high

0148-0227/03/2003JA009915

latitudes and the dayside dip equator by *Nishida et al.* [1966] and *Nishida* [1968a]. The coherent polar and equatorial *DP* 2 was controlled by the southward interplanetary magnetic field [*Nishida*, 1968b]. *Kikuchi et al.* [1996] demonstrated the extremely high coherency between the auroral and equatorial *DP* 2 by using data of the European Incoherent Scatter (EISCAT) measurement of the convection electric field and of the high time resolution magnetometer array from the auroral to equatorial latitudes. *Kikuchi et al.* [1996] concluded that the high latitude *DP* 2 was caused by the ionospheric Hall currents driven by the convection electric field and that the convection electric field propagated to the equator nearly instantaneously within a temporal resolution of 25 s. As a result, the equatorial *DP* 2 was caused by the Pedersen currents amplified by the Cowling effect, connecting with the R1 FACs through the mid latitude ionosphere [*Kikuchi et al.*, 1996].

[4] During a period of southward IMF, the development of the partial ring current causes a shielding effect on the penetrated convection electric field [*Vasyliunas*, 1972; *Jaggi and Wolf*, 1973; *Crooker and Siscoe*, 1981; *Senior and Blanc*, 1984]. The shielding electric field causes an intensification of the convection electric field at auroral latitudes, resulting in the intensification of the eastward auroral electrojet of the *DP* 1 current in the afternoon to evening sectors [*Iijima and Nagata*, 1972]. The time constant for the shielding effect being effective at low latitudes was estimated to be 20 min [*Somayajulu et al.*, 1987] and 17 min [*Kikuchi et al.*, 2000b] based on the magnetometer observations, and around 20 min based on model calculations depending on the density and temperature of the plasma sheet [*Senior and Blanc*, 1984; *Peymirat et al.*, 2000]. An overshielding effect occurs, when the convection electric field decreased abruptly because of the northward turning of the Interplanetary Magnetic Field (IMF) [*Fejer et al.*, 1979; *Kelley et al.*, 1979; *Gonzales et al.*, 1979, 1983]. *Gonzales et al.* [1979] demonstrated that the Jicamarca incoherent scatter radar detected an increase in the ionospheric electric field during the night, opposite in direction to the convection electric field. *Rastogi* [1977] found that the northward turning of the IMF caused substantial decreases in the electric field and electrojet at the dayside equator during a geomagnetic storm. *Reddy et al.* [1979, 1981] measured a westward electric field in the daytime equatorial ionosphere with VHF backscatter radar during a substorm. The overshielding effect reduces the intensity of the equatorial electrojet on the dayside [*Kobea et al.*, 1998, 2000; *Kikuchi et al.*, 2000a, 2000b]. As a result, the negative magnetic bay associated with a substorm decreased its amplitude with latitude, but was enhanced considerably at the dayside dip equator when the ionospheric convection electric field decreased abruptly, as observed by the EISCAT radar and the auroral-to-equatorial magnetometer arrays [*Kikuchi et al.*, 2000b]. *Kikuchi et al.* [2000b] quantitatively deduced the overshielding electric field that overcame the convection electric field around the peak of the negative bay because of the time delay of its growth (17 min). They further suggested that the R2 FACs flowed into the dayside equatorial ionosphere, causing negative magnetic perturbations superposed on the negative bay that was due to the partial ring current in the magnetosphere. These observations enable us to extend the *DP* 1 currents to mid and low latitudes, particularly to the dayside dip equator. *Kikuchi et al.* [2000a] pointed out that the enhanced negative bay at the equator could appear as the equatorial CEJ, and suggested that the northward turning of the IMF caused the equatorial CEJ under the condition of well-developed R2 FACs.

[5] One of the purposes of this paper is to confirm the scenario for the equatorial CEJ associated with the substorm as a manifestation of the overshielding effects due to the R2 FACs that become dominant when the R1 FACs are depressed abruptly by the northward turning of the IMF. We have completed a detailed analysis of the event reported by *Kikuchi et al.* [2000a] by focusing on the IMF-dependent development and decay of the polar cap potential (PCP) and on the ground magnetic signatures of the dominant R2 FACs during the equatorial CEJ. With this scenario, we propose a model of the *DP* 1 current system in the dayside ionosphere including the equator, which is a combination of the *DP* 2 currents due to the R1 FACs with reversed ionospheric currents due to the R2 FACs that overcome the R1 FACs when the R1 FACs decay rapidly because of the northward turning of the IMF.

[6] Another important issue is how one should explain the instantaneous transmission of the ionospheric electric field and current associated with the R1 and R2 FACs from the polar ionosphere to the equatorial ionosphere. *Kikuchi et al.* [1978] and *Kikuchi and Araki* [1979b] proposed the Earth-ionosphere waveguide model for the instantaneous transmission of the electric field to the equator. The zeroth-order transverse magnetic (TM) mode propagates in the waveguide at the speed of light, accompanying electric currents in the conducting ionosphere. Once the polar electric field has propagated to the low-latitude ionosphere, one can calculate the distribution of the electric field and current in the ionosphere by assuming an electric potential drop in the polar ionosphere [*Tsunomura and Araki*, 1984]. The waveguide model further predicts that the electric field in the conducting ionosphere is transmitted upward to the ionospheric *F* region at mid and low latitudes along the magnetic field lines [*Kikuchi and Araki*, 1979b]. In order to apply the Earth-ionosphere waveguide model to the CEJ events, we need to reveal that the electric field in the ionospheric *F* region is coherent with the ionospheric current at the equator.

[7] In the latter part of the present paper, we analyze another CEJ event that occurred on 8 April 1993 and demonstrate that the electric field in the equatorial *F* region measured by the Jicamarca incoherent scatter radar is coherent with the equatorial CEJ recorded near the radar, in agreement with the Earth-ionosphere waveguide model of *Kikuchi and Araki* [1979b].

2. Observation

2.1. CEJ Event on 16 July 1995

2.1.1. Development of R1 and R2 FACs

[8] The interplanetary magnetic field (IMF) observed by Wind (x = 171 R_E) turned southward at 1227 UT and returned to a positive value at 1505 UT on 16 July 1995 as indicated in Figure 1. The southward turning of the IMF caused the growth of R1 FACs, which in turn enhanced the polar cap potential (PCP) at 1313 UT as manifested by a

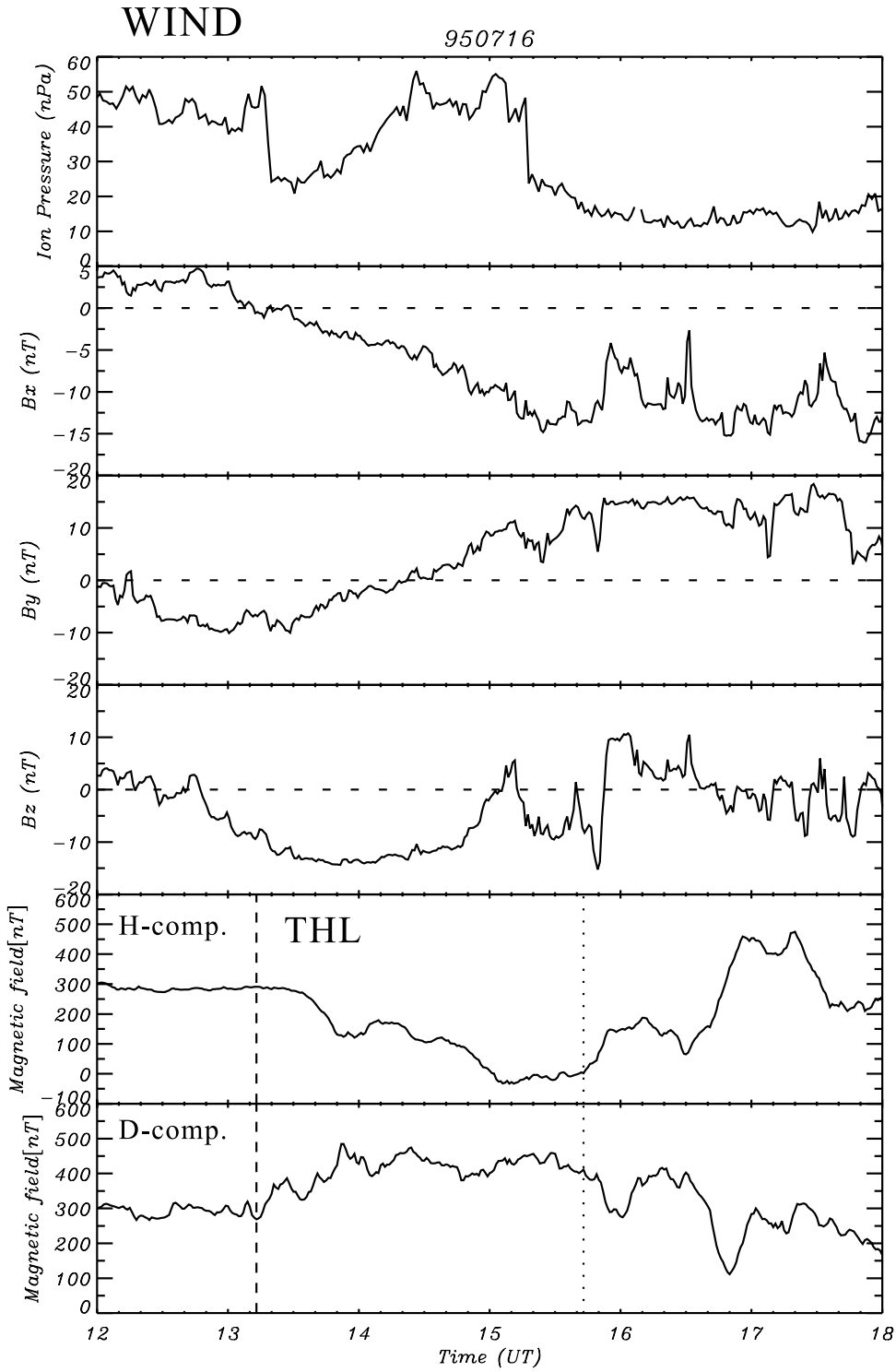

Figure 1. Three components of the interplanetary magnetic field measured by Wind ($x = 171\ R_E$), and H and D components of the magnetic field recorded at the polar cap station, Thule. The increase in the D component at 1313 UT (dashed line) indicates a growth of the polar cap potential initiated by the southward turning of the IMF at 1227 UT. The increase in the H component at 1543 UT (dotted line) indicates the decay of the polar cap potential due to the northward turning of the IMF at 1505 UT.

decrease in the H and an increase in the D component of the magnetic field at Thule (THL, 85.58°N in corrected geomagnetic coordinates (CGM)) that was located at 1000 magnetic local time (MLT) in the polar cap as shown in Figure 1 (vertical dashed line). The coordinates of all the magnetometer stations used in this paper are listed in Table 1. The increase in the PCP also caused a gradual magnetic field decrease at Ny Alesund (NAL, 76.03°N

Table 1. List of the IMAGE, CANOPUS, INTERMAGNET, and Brazilian Magnetometer Stations

Station	Geographic Latitude	Geographic Longitude	Corrected Geomagnetic Latitude	Corrected Geomagnetic Longitude	Dip Latitude	MLT (UT+)
			IMAGE			
NAL, Ny Alesund	78.92	11.95	76.03	112.45		+3.2
HOR, Hornsund	77.00	15.60	73.98	110.61		+3.1
HOP, Hopen Island	76.51	25.01	72.87	115.94		+3.5
BJN, Bear Island	74.50	19.20	71.30	108.93		+3.1
SOR, Soroya	70.54	22.22	67.22	106.84		+2.9
MAS, Masi	69.46	23.70	66.05	107.02		+2.9
KEV, Kevo	69.76	27.00	66.18	109.82		+3.1
TRO, Tromsø	69.66	18.94	66.53	103.57		+2.7
KIL, Kilpisjarvi	69.02	20.79	65.76	104.42		+2.8
MUO, Muonio	68.02	23.53	64.60	105.79		+2.9
PEL, Pello	66.90	24.08	63.44	105.45		+2.8
OUJ, Oulujarvi	64.52	27.23	60.87	106.58		+2.9
HAN, Hankasalmi	62.30	26.65	58.60	105.01		+2.8
NUR, Nurmijarvi	60.50	24.65	56.80	102.55		+2.7
			CANOPUS			
RAN, Rankin	62.82	267.89	73.18	333.92		−6.5
ESK, Eskimo Point	61.11	265.95	71.46	331.04		−6.6
CHU, Fort Churchill	58.76	265.92	69.25	331.57		−6.6
GIL, Gillam	56.38	265.36	66.93	331.16		−6.6
ISL, Island Lake	53.86	265.34	64.49	331.56		−6.6
PIN, Pinawa	50.20	263.96	60.76	330.03		−6.7
			INTERMAGNET			
THL, Thule	77.48	290.83	85.58	34.29		−2.9
			EMN (*Brazilian Zone*)			
ANC, Ancon	−11.79	282.84	3.05	354.40	0.7	−5.1
GLP, Guadalupe	−14.06	−75.95	−0.06	355.57	−1.5	−5.1
BLM, Belem	−1.22	−48.53	1.73	25.51	7.1	−3.2
SLZ, Sao Luis	−2.60	−44.20	0.47	29.56	−0.2	−3.0
EUS, Eusebio	−3.85	−38.42	0.11	34.70	−9.3	−2.4
SMA, Santa Maria	−29.72	−53.72	−19.07	13.19	−32.6	−4.0

CGM) as shown in Figure 2, which started at 1313 UT (vertical dashed line) when the station was located in the afternoon sector (1600 MLT). These magnetic perturbations match the *DP* 2 Hall currents driven by the dawn-dusk convection electric field. The *DP* 2 currents at auroral to midlatitudes in the afternoon sector caused an increase in the *X* component of the magnetic field from Hornsund (HOR) to Nurmijarvi (NUR) (74°–56°N CGM) (Figure 2). These magnetic field disturbances are a result of the ionospheric convection whose direction is antisunward in the polar cap and sunward at auroral to mid latitudes in the afternoon sector. It should be noted that the magnetic field disturbances at the polar cap, auroral and midlatitude stations started simultaneously at 1313 UT as shown by the dashed line. This implies an instantaneous development of Hall currents due to a divergent electric field surrounding the R1 FACs, which propagated nearly instantaneously to the midlatitude. The northward turning of the IMF, on the other hand, caused a decrease in the R1 FACs at 1543 UT, as manifested by the increases in the *H* component of the magnetic field at Thule as shown by the dotted line in Figure 1 and in the *X* component at NAL (Figure 2). The *X* component of the magnetic field at auroral to midlatitudes decreased with the decrease in the PCP as shown by the dotted line in Figure 2. This again implies instantaneous propagation of the convection electric field to the midlatitude.

[9] The Los Alamos National Laboratory (LANL) 1994-084 satellite (data not shown here) detected an injection of hot plasma at 1455 UT in the 0200 MLT meridian, indicating an onset of the substorm. Negative bay signatures were observed at the Canadian Auroral Network for the OPEN Program Unified Study (CANOPUS) magnetometer stations in the morning sector, as shown in Figure 3. The sudden onset of the negative bay at Eskimo Point (ESK, 71.46°N CGM) and Rankin Inlet (RAN, 73.18°N CGM) starting at 1455 UT coincided with the injection detected by the LANL particle detector. Figure 4 shows the *X* component of the magnetic field at three stations at Oulujarvi (OUJ, 60.87°N CGM), Hankasalmi (HAN, 58.60°N CGM), and Nurmijarvi (NUR, 56.80°N CGM) extracted from Figure 2, to indicate the distinct feature of the ionospheric current at midlatitude from the eastward electrojet at auroral latitudes. During the substorm (1500–1600 UT), the eastward electrojet intensified considerably in the afternoon sector as seen at OUJ and started to decay at around 1543 UT (vertical dotted line). The significant intensification of the eastward electrojet at OUJ may have been caused by increased conductivity, which was not recognized at the midlatitude station, NUR. It should be noted that the decrease in the eastward electrojet at 1543 UT occurred in concert with the decrease in the eastward current at HAN and NUR, and also with the decrease in the PCP at 1543 UT (Figure 1). This coherency indicates a decrease in the convection electric field penetrating from the polar cap to midlatitudes. It should be noted that the *X* component of the magnetic field at NUR was far below the preevent level (horizontal

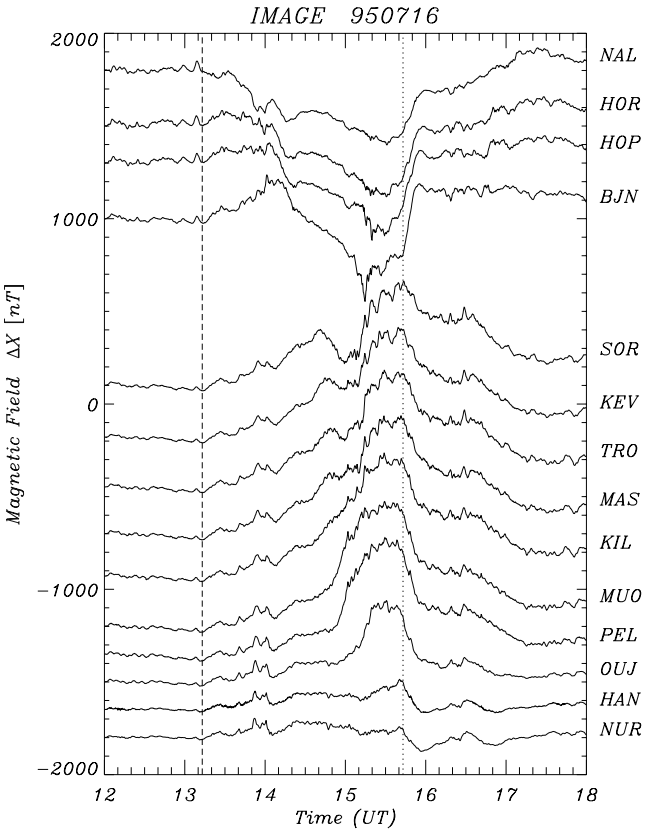

Figure 2. *X* component of the magnetic field recorded at the IMAGE magnetometer stations located in the afternoon sector during the substorm cycle. The growth of the polar cap potential starting at 1313 UT is recognized as the gradual enhancement of the eastward electrojet at auroral and mid latitudes (dashed line). The rapid recovery of the electrojet at 1543 UT (dotted line) represents the decay of the polar cap potential due to the northward turning of the IMF.

dashed line), while it remained at the preevent level at HAN and at a higher level at OUJ. If we draw an equivalent current vector for the *X* component of the magnetic field at 1600 UT, the vector is eastward at OUJ and null at HAN, but westward at NUR. It should be recalled that the *X* component of the magnetic field at these three stations was intensified coherently at 1313 UT by the southward turning of the IMF (vertical dashed line). The reversed current at NUR that was coherent with the decrease in the PCP has probably been caused by R2 FACs, which developed after the growth of the R1 FACs. This is another example of the overshielding effect due to the R2 FACs as suggested by *Kikuchi et al.* [2000b]. It is important to note that the reversed current over NUR is not a "return current" of the eastward auroral electrojet (e.g., OUJ). The EISCAT and magnetometer array observations revealed that the eastward auroral electrojet in the afternoon sector and the reversed currents equatorward of the electrojet were primarily the Hall currents driven by the electric field associated with the R1 and R2 FACs [*Kikuchi et al.*, 2000b]. In particular, the reversed currents at mid latitudes can be explained if we assume that the Hall currents were driven by the divergent electric field surrounding the R2 FACs.

2.1.2. Equatorial CEJ

[10] As indicated in Figure 5, the *H* component of the magnetic field at the equatorial stations, Guadalupe (GLP, −1.5° dip latitude (DLAT)) and Ancon (ANC, 0.7° DLAT) in Peru, resemble those at NUR over the interval 1300–1700 UT. Figure 5 also shows that the amplitude of the magnetic perturbations is much larger at the equatorial stations, GLP and ANC, than that at low-latitude stations, Eusebio (EUS, −9.3° DLAT) and Santa Maria (SMA, −32.6° DLAT, 19.07°S CGM). The equatorial enhancement of the amplitude suggests a major contribution of ionospheric currents rather than currents in the magnetosphere. This further suggests that the polar electric field penetrated to low latitudes with decreasing amplitude because of the geometrical attenuation [*Kikuchi et al.*, 1978], but drove considerable currents in the equatorial ionosphere with the aid of the Cowling effect. Thus the onsets of the increase in the electric field at 1313 UT at auroral and equatorial latitudes are simultaneous, in agreement with the instantaneous penetration of the convection electric field to low latitudes during quasiperiodic *DP* 2 events, as shown by *Kikuchi et al.* [1996].

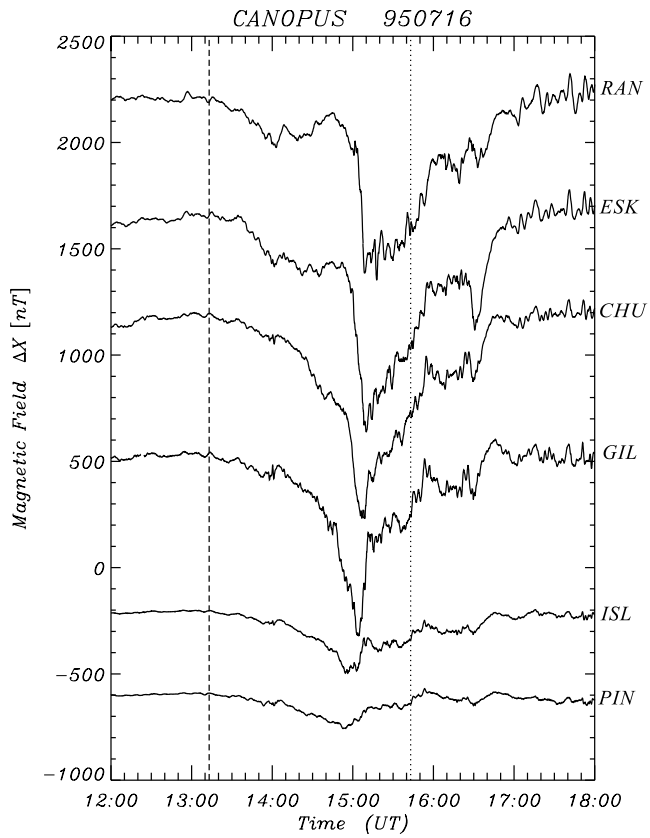

Figure 3. *X* component of the magnetic field recorded at the CANOPUS magnetometer stations located in the morning sector during the substorm cycle. The growth of the polar cap potential starting at 1313 UT is recognized as the gradual enhancement of the westward electrojet (dashed line).

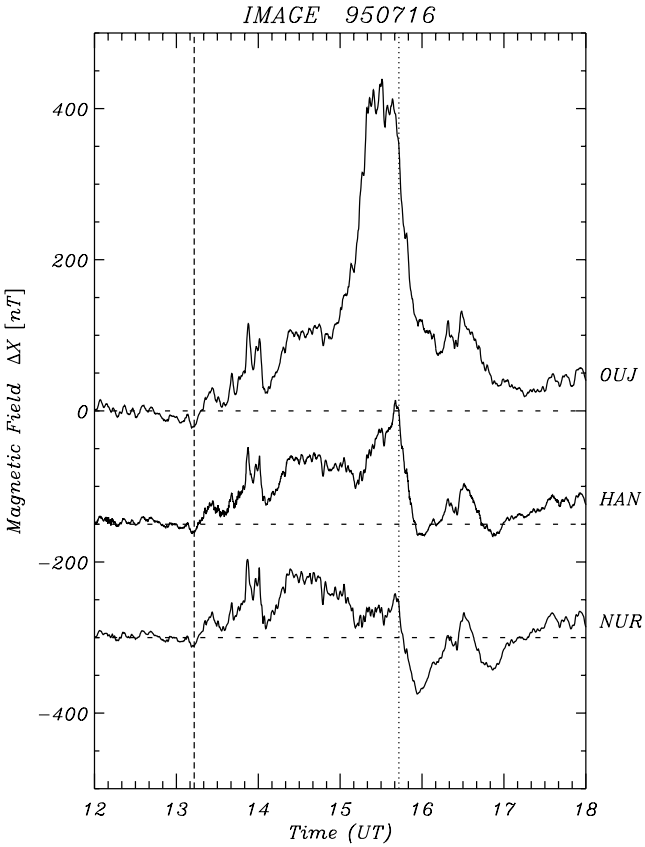

Figure 4. *X* component of the magnetic field recorded at the mid latitude (NUR) as well as the auroral latitude (HAN, OUJ). The *X* component at NUR started to increase in concert with the growth of the eastward electrojet at OUJ (vertical dashed line) but decreased substantially at 1543 UT (dotted line) to be well below the preevent level (horizontal dashed line), while the *X* component was well above the preevent level at OUJ.

[11] The *H* component of the magnetic field at GLP and ANC started to decrease at 1543 UT, attaining a peak at 1557 UT. It recovered to the quiet time daily level at 1630 UT (Figure 5). Here, we note that the *H* component of the magnetic field near the dip equator decreased considerably with respect to the magnetic disturbances at the low latitudes. The amplitude of the magnetic field decrease measured from the beginning of the CEJ to the peak is 80 nT at ANC, being comparable to or even larger than the size of the diurnal variation over the time interval 1200–1500 UT. No magnetic field depression was observed at low latitude stations, EUS and SMA. The equatorial enhancement of the magnetic field decrease suggests again that an intense westward electrojet was driven in the equatorial ionosphere, being superposed on the normal eastward electrojet at the equator in a similar way to the enhanced eastward electrojet during the *DP* 2 events. As a result, the *H* component of the magnetic field was well below the nighttime level at the equatorial stations, which is identified here as the equatorial counterelectrojet (CEJ). This behavior is similar to that at NUR (Figure 4).

[12] The resemblance between the midlatitude and equatorial magnetic field variations suggests that the electric field associated with the R2 FACs penetrated to the equator as well as to the midlatitude, as suggested by *Kikuchi et al.* [2000b]. From the electric current point of view, the R2 FACs flow into the equatorial ionosphere through the midlatitude ionosphere. A possible corresponding signature in the solar wind parameters is the northward turning of the IMF that occurred at 1505 UT (Figure 1) at the position of the satellite, which caused the abrupt decrease in the R1 FAC as manifested by the polar cap magnetometer (dotted line in Figure 1) if the travel time to the Earth is taken into account. The electric field decreased to the presubstorm level at auroral latitudes at 1557 UT, 15 min after the onset of the decrease in the R1 FACs. Thus we suggest that the equatorial CEJ was caused by the R2 FACs, which overcame the R1 FACs when the R1 FACs decayed rapidly because of the northward turning of the IMF.

2.2. CEJ Event on 8 April 1993

2.2.1. Polar Cap Potential

[13] In this section, we provide direct evidence of the electric field responsible for the equatorial CEJ. Figure 6 shows solar wind parameters measured by IMP 8 ($x = 0$, $y = -20$, $z = -30\ R_E$) over an interval, 1610–1815 UT. During 1610–1745 UT, the IMF was southward and had a relatively constant amplitude of 5–7 nT. The IMF started to

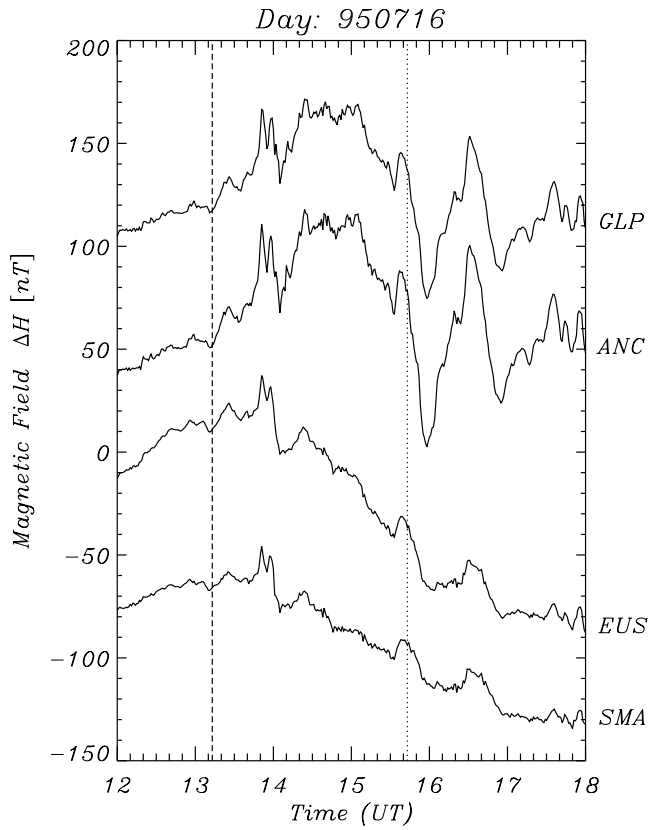

Figure 5. *H* component of the magnetic field recorded at low latitudes and near the dip equator in Peru and Brazil. The *H* component started to increase gradually at 1313 UT (dashed line) in correspondence with the growth of the polar cap potential, while the counterelectrojet is observed at the dip equator in correspondence with the decrease in the polar cap potential starting at 1543 UT (dotted line).

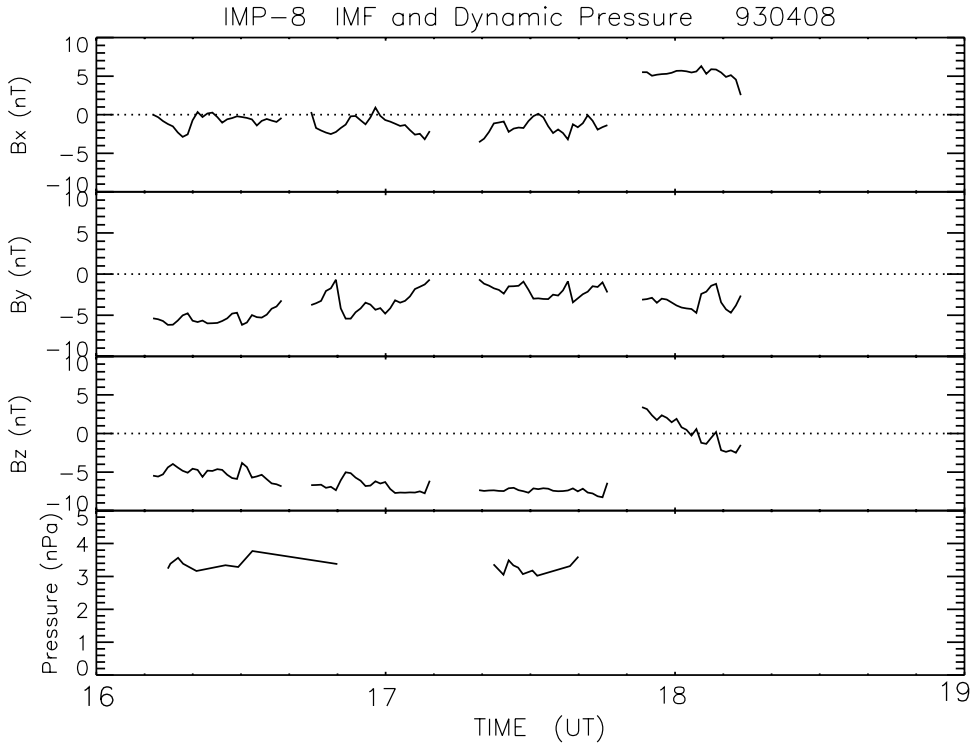

Figure 6. Interplanetary magnetic field and solar wind dynamic pressure observed by IMP 8 located at ($x = 0$, $y = -20$, $z = -30$ R_E in GSM coordinate). The IMF started to turn northward at 1745 UT and became positive by 1752 UT. The northward turning may have occurred at around 1750 UT.

turn northward at 1745 UT, and became positive by 1752 UT, although there was a data gap between these times. If we interpolate the data for the data gap period, $Bz > 0$ occurred at about 1750 UT. Since IMP 8 was located at $x = 0$, the northward turning of IMF must have occurred at the subsolar point of the magnetopause a few minutes before 1750 UT.

[14] Figure 7 shows the H and D components of the magnetic field at Thule, indicating development of the PCP during the time interval shown. In particular, the H component of the magnetic field abruptly increased at 1750 UT as shown by the vertical dotted line, indicating an abrupt decrease in the PCP. The D component at Resolute Bay (83.0° GML, data not shown) decreased by 160 nT at 1750 UT, indicating a decrease in the poleward flow around the cusp. The decrease in the PCP must have been caused by the northward turning of the IMF a few minutes before 1750 UT (Figure 6).

[15] Figure 8 shows the X component of the magnetic field at OUJ, HAN and NUR over the interval 0000–2400 UT. One can see that the perturbations at the auroral stations are in antiphase to those in the polar cap over the interval 1200–1800 UT. In particular, the quasi-periodic fluctuations with the period of 1.5 hours are coherent in the polar cap, auroral and midlatitudes, suggesting a global extension of the convection electric field. However, no decrease in the auroral electrojet corresponded to the decrease in the PCP at 1750 UT, probably caused by some disturbances associated with the substorm.

2.2.2. Equatorial CEJ

[16] Figure 9 shows the H component of the magnetic field at low and equatorial latitudes, ANC, Peru, and Belem (BLM, 7.1° DLAT), Sao Luis (SLZ, −0.2° DLAT), Eusebio (EUS, −9.3° DLAT), and SMA, Brazil on the disturbed day (solid curves) and on the quiet day (dotted curve) (no data for EUS). Quasiperiodic fluctuations with a period of 1.5 hours are observed at all stations over the interval 1200–1800 UT, but the amplitude is significantly enhanced

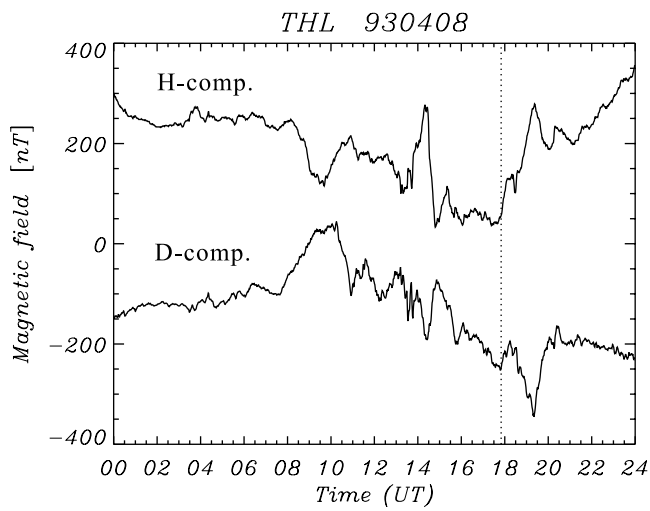

Figure 7. H and D components of the magnetic field recorded at Thule on 8 April 1993. The H component substantially increased at 1750 UT (dotted line) after showing quasiperiodic fluctuations, which may indicate the rapid decay of the polar cap potential due to the northward turning of the IMF.

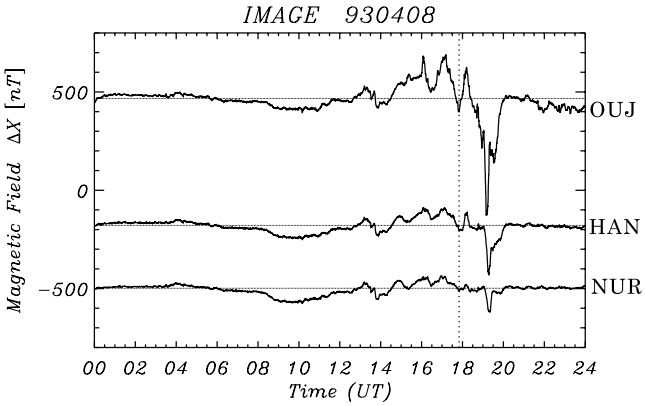

Figure 8. *X* component of the magnetic field at auroral to mid latitude stations, OUJ, HAN, and NUR located in the afternoon to evening sectors. The quasiperiodic fluctuations with a period of 1.5 hours correspond to those observed in the polar cap potential, although no appreciable changes are recognized in correspondence to the decay of the polar cap potential (dotted line).

near the dip equator, SLZ. The equatorial enhancement of the quasiperiodic fluctuations suggest that the electric field propagated from the polar ionosphere to the equator. Indeed, similar quasiperiodic fluctuations were recorded on the *H* component at Thule (Figure 7) and at auroral to midlatitude stations (Figure 8). The coherent magnetic fluctuations from the polar cap to the equator should be identified as the *DP* 2 [*Nishida et al.*, 1966]; that is, the *DP* 2 currents originating in the polar ionosphere expanded instantaneously to the dayside equator where the current is amplified by the Cowling effect. *Kikuchi et al.* [1996] demonstrated that the *DP* 2 magnetic fluctuations at high and equatorial latitudes appeared simultaneously if we allow for the temporal resolution of 25 s. The simultaneous occurrence can be explained by the Earth-ionosphere waveguide model as suggested by *Kikuchi et al.* [1978] and *Kikuchi and Araki* [1979b], which explained the simultaneous onset of the PRI of the SC [*Araki*, 1977]. The transmitted electric field suffers from geometrical attenuation, reducing the amplitude of the *DP* 2 at low latitudes, but driving significant currents at the dayside dip equator because of the Cowling effect [*Kikuchi et al.*, 1978]. As a result, the amplitude of the *DP* 2 magnetic fluctuation is a few times greater than that at low latitude [*Nishida*, 1968a; *Kikuchi et al.*, 1996]. It is apparent that the *DP* 2 fluctuation shown in Figure 9 is enhanced at the dip equator (SLZ) comparing with low latitudes (e.g., SMA). It is interesting to note that the amplitude of the *DP* 2 magnetic fluctuation at around 1600 UT is well above the quiet time daily level (dashed line) at ANC, Peru, but it is below the quiet time level at SLZ, Brazil. This distinct local time feature is consistent with the *DP* 2 [*Kikuchi et al.*, 1996], which suggests larger amplitude of the penetrated electric field in the morning (1100 MLT at ANC) than in the afternoon (1300 MLT at SLZ) sector. This tendency is also consistent with the Jicamarca incoherent scatter radar observation [*Fejer*, 1991] and model calculations [*Tsunomura and Araki*, 1984; *Senior and Blanc*, 1984].

[17] A steep magnetic decrease started at 1750 UT (Figure 9), in correspondence to the decrease in the PCP shown in Figure 7. It should be noted that the decrease in the magnetic field during 1750–1920 UT is well under the nighttime magnetic level, with an amplitude of 65 nT at SLZ (1500 MLT), as measured from the value at around 2100 UT. This decrease is identified as the equatorial CEJ in the same way as in the previous event. The *H* component of the magnetic field at ANC (1300 MLT) was well below the quiet daily variation (dotted curve), but remained above the nighttime level, since it occurred when the background eastward electrojet was stronger than the CEJ. Thus the equatorial CEJ appeared at the Brazilian station that was located in the afternoon sector (1500 MLT), while substantial reversed currents of a magnitude comparable to the normal diurnal variation were superimposed on the daily equatorial eastward electrojet at ANC in the postnoon (1300 MLT).

2.2.3. Electric Field at Jicamarca

[18] Figure 10 shows the vertical velocity of the ionospheric plasma measured by the Jicamarca incoherent scatter radar (11°57′S, 76°52′W; magnetic dip 2°N), with the time resolution of 5 min. The vertical motion of plasma having a velocity of 40 m/s gives an electric field of 1 mV/m, and the resolution is 2 m/s (0.05 mV/m) [*Fejer*, 1991]. In Figure 10, the averaged quiet day curve (QDC) is shown with the dashed curve, for the purpose of comparison with the disturbed day (solid curve). Unfortunately the radar data is not available for times after 1822 UT, but the available data includes the maximum intensity of the equatorial CEJ. The electric field deduced from the plasma drift speed is positive during most of the time period, but went down below the quiet time level at around 1800 UT as indicated with the dashed curve in Figure 10, suggesting a reversed electric field superposed on the quiet time electric field. It is observed that the temporal variation of the electric field in the *F* region is in coincidence with the magnetic variations recorded at ANC (Figure 9). The correlation coefficient between the electric field at Jicamarca and magnetic field at ANC is 0.97 for the period 1331–1822 UT. The electric field change is also coherent with magnetic variations at NUR (Figure 8) with a correlation coefficient of 0.90 for the time interval 1331–1600 UT. The good correlation between the equatorial electric field and the ionospheric current extending from high latitudes to the equator would give us an idea about the mechanism for the transmission of the polar electric field to the equator, as discussed later.

[19] The electric field measured by the Jicamarca radar decreased steeply at around 1800 UT corresponding to the equatorial CEJ (vertical dotted line). The coherency between the decrease in the PCP and the CEJ suggests again that the decrease in the polar electric field propagated down to the equator nearly instantaneously. It should be noted that the PCP decreased its intensity during the CEJ event, but the convection electric field in the polar cap remained in the dawn-to-dusk direction. If we assume that the convection electric field penetrated to the equator without accompanying the shielding electric field, one would find that the vertical drift velocity decreased but remained above the quiet time curve at around 1800 UT. In contrast, the radar observation indicated that the equatorial electric field went

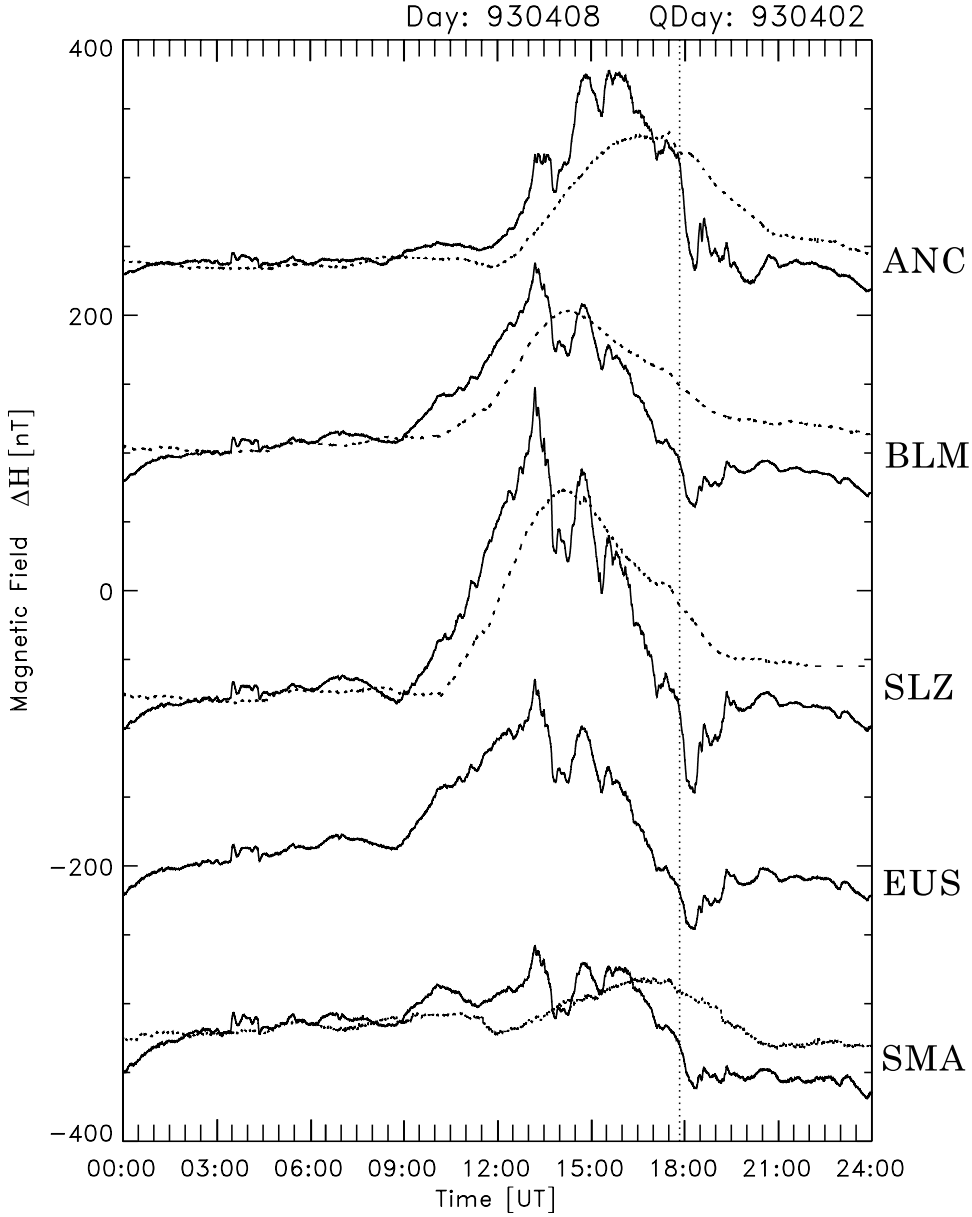

Figure 9. *H* component of the magnetic field at low and equatorial latitudes (solid curves). The dotted curves refer to the quiet-day diurnal curve on 2 April 1993 (no data for EUS). The quasiperiodic fluctuations are significantly enhanced at the dip equator (ANC, SLZ) with respect to those at low latitude (SMA). The decrease in the *H* component at 1750 UT (dotted line) is enhanced considerably to appear as the equatorial CEJ.

below the quiet time level (Figure 10). The reversed electric field relative to the quiet time curve is considered to be an overshielding electric field due to the R2 FACs as suggested by *Kikuchi et al.* [2000b].

3. Summary and Discussion

3.1. DP1 Current System

[20] A rapid change in the convection electric field can penetrate to the equator with no significant shielding effect, since the R2 FAC develops with a time delay of tens of min [*Somayajulu et al.*, 1987; *Kikuchi et al.*, 2000b]. The *DP* 2 ionospheric current is primarily composed of Hall currents surrounding the R1 FACs at high latitudes and of the Pedersen currents amplified by the Cowling effect at the dayside dip equator [*Kikuchi et al.*, 1996]. The Hall current closes in the ionosphere if we assume uniform ionospheric conductivity, while the Pedersen current must be connected to the R1 FACs.

[21] The growth of the magnetospheric convection would cause development of the ring current, and in turn develop the R2 FACs flowing into the evening-to-afternoon auroral ionosphere [*Vasyliunas*, 1972]. The R2 FACs make a shielding effect so as to cancel the convection electric field at low latitudes. The time constant of the growth of the R2 FACs is estimated theoretically as being of the

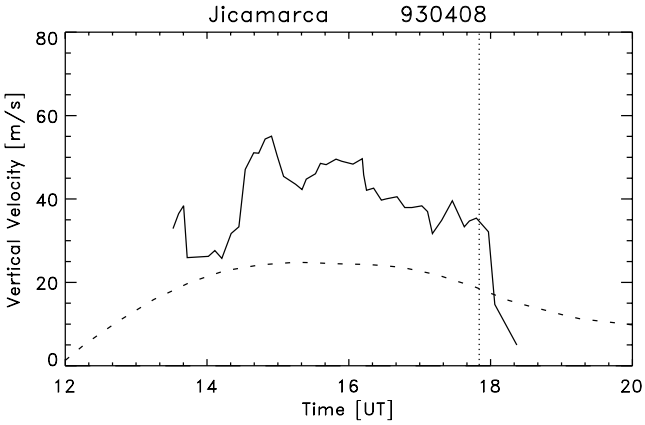

Figure 10. Vertical drift velocity of the ionospheric plasma observed by the Jicamarca incoherent scatter radar for the disturbed day (solid curve) and for the quiet time daily variations (dashed curve). The velocity of 40 m/s corresponds to the electric field of 1 mV/m. The quasiperiodic fluctuations are coherent with those observed in the polar cap and auroral to mid latitudes. The rapid decrease starting at 1750 UT (dotted line) in the electric field corresponds to the equatorial CEJ and to the decrease in the polar cap potential.

order of tens of min, which depends on the density and temperature of the plasma sheet [*Senior and Blanc*, 1984; *Spiro et al.*, 1988]. The magnetometer and radar observation suggest the same order of time constant for the shielding effect [*Somayajulu et al.*, 1987; *Kikuchi et al.*, 2000b].

[22] If the R1 FACs decrease so rapidly that the R2 FACs cannot follow the change in the penetrating electric field, the electric field at the mid latitudes and the dayside equator is reversed from eastward to westward because of the dominant shielding electric field [*Kelley et al.*, 1979]. *Peymirat et al.* [2000] demonstrated that the sudden decrease in the polar cap potential produced dramatic change in the direction of the equatorial electric field due to the R2 FACs using the Magnetosphere-Thermosphere-Ionosphere-Electrodynamics General Circulation Model (MTIEGCM) of *Peymirat et al.* [1998]. Thus the magnetic field is depressed well below the nighttime level at mid latitudes and the dayside dip equator as demonstrated above (Figures 4, 5, and 9). Since the time constant for the development of the shielding electric field is of the order of tens of min, the shielding electric field would play a major role for several tens of min after the polar cap potential deceases suddenly. *Kikuchi et al.* [2000b] revealed that the shielding electric field associated with the R2 FAC developed with a time delay of 17 min from the growth of the R1 FAC, and that it was the predominant contribution around the peak of the negative bay at the dayside dip equator. As a result, the negative bay was considerably enhanced at the dayside dip equator. The enhanced negative bay appeared as the equatorial CEJ. The electric field in the polar cap is rapidly reduced when the IMF turns northward [e.g., *Sergeev et al.*, 1986]. We have shown above that the abrupt decrease in the PCP corresponded to the northward turning of the IMF. In the second CEJ event analyzed above, the Jicamarca radar directly detected the rapid decrease in the eastward electric field, suggesting the reversed electric field superimposed on the eastward dynamo electric field.

[23] We here make a brief comment on the relation between the equatorial CEJ and the phase of the substorm. Quite a few substorms are triggered by the northward turning of the IMF [*Rostoker et al.*, 1980; *Lyons*, 1995]. In the first event analyzed, the substorm commenced at around 1455 UT on 16 July 1995, as determined by the injection of energetic particles in 0200 MLT and by a sudden onset of absorption in the morning sector [*Kikuchi et al.*, 2000a]. There is no clear signature in the IMF that triggered the substorm, although the *H* component of the magnetic field at Thule changed its temporal behavior from the steep decrease to a gradual increase at the onset of the substorm (Figure 1). The significant change in the polar cap potential may be related to the substorm onset, but it did not make any effect on the equatorial electrojet. The equatorial CEJ took place in the recovery phase of the substorm, when the polar cap potential decreased substantially because of the northward turning of the IMF. This implies that the R2 FACs have been fully developed during the substorm so that they can produce the CEJ when the PCP decreased abruptly as suggested by *Kikuchi et al.* [2000b]. The second CEJ event also occurred late during the recovery phase of the substorm as apparently seen on the AE index (WDC-C2 for Geomagnetism, Kyoto University, http://swdcdb.kugi.kyoto-u.ac.jp/). The IMF data is not available for the time corresponding to the onset of the substorm, but the southward IMF (Figure 6) before the CEJ may have developed the R2 FACs during the substorm.

[24] As shown above, the CEJ is an additional westward current overcoming the eastward dynamo current. Most probable candidate for the additional current is the R2 FAC as suggested by *Kikuchi et al.* [2000b]. The R2 FACs intensify the eastward auroral electrojet combined with the R1 FACs, while they produce reversed currents at lower latitudes. The intensified eastward auroral electrojet is an afternoon portion of the *DP* 1 currents [*Iijima and Nagata*, 1972]. The R2 FACs cause the shielding effect on the penetrated electric field, but become dominant when the R1 FACs decay rapidly because of the northward turning of the IMF. Here we define two phases of the *DP* 1 current in the dayside ionosphere. One is characterized by shielding (*DP* 1–1), and the other is overshielding (*DP* 1–2). During the *DP* 1–2 period, the *DP* 1 current is composed of the Hall currents surrounding the R2 FACs at midlatitudes and the CEJ at the dayside dip equator, as indicated with the schematic diagram in Figure 11. The ionospheric current system must have a current source in the magnetosphere. *Tanaka* [1995], using MHD simulations, revealed that the high-pressure plasma was accumulated around the cusp, which would generate a perpendicular current in the high latitude boundary layer feeding the R1 FACs. The current generator would also feed the ionospheric currents including the *DP* 2 currents along the dayside dip equator, if we apply the current system between the magnetosphere and ionosphere for the *DP* 2 [*Kikuchi et al.*, 1996]. The CEJ, on the other hand, is primarily composed of the reversed currents connecting with the R2 FACs as suggested by *Kikuchi et al.* [2000b]. Thus the equatorial CEJ is fed by the current generator in the inner

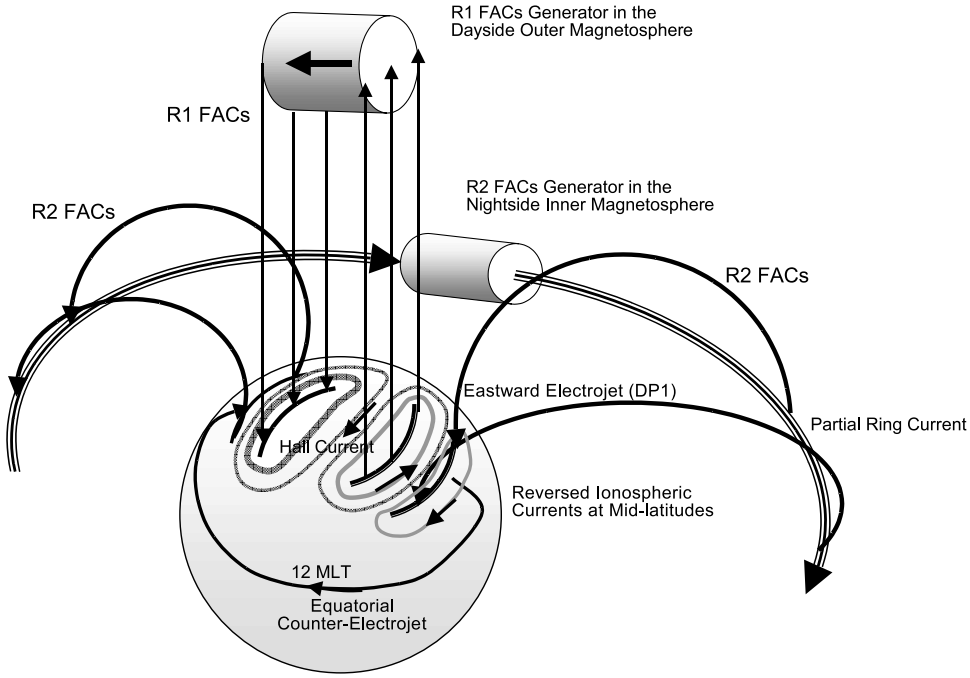

Figure 11. Schematic diagram of the current system in the magnetosphere and ionosphere during the substorm. The R1 and R2 FACs flow into the equatorial ionosphere through the polar ionosphere, resulting in the equatorial *DP* 2 when the R1 FACs are dominant, while the equatorial CEJ appears when the R1 FACs decay rapidly because of the northward turning of the IMF. The diagram is pertinent to the equatorial CEJ.

magnetosphere [*Vasyliunas*, 1972], as schematically shown in Figure 11.

3.2. Instantaneous Transmission to the Equator

[25] One of our concerns is how the electric field is transmitted to the equatorial ionosphere nearly instantaneously so as to drive the Pedersen current in the *E* region at the dayside dip equator. Another issue is how to drive the vertical motion of the *F* region plasma at the equator, as observed by the Jicamarca radar. Instantaneous penetration of the high-latitude electric field to the equator has been suggested for rapid magnetic changes such as the geomagnetic sudden commencement (SC) based on the simultaneous onset of the preliminary reverse impulse (PRI) at afternoon high latitudes and at the dayside dip equator [*Araki*, 1977]. HF Doppler observations detected the instantaneously transmitted electric field at low latitude coherent with the high latitude PRI [*Kikuchi*, 1986]. *Kikuchi* [1986] pointed out that the *F* region electric field as well as the *E* region current could be explained by the Earth-ionosphere waveguide model. The convection electric field also penetrates to the equator nearly instantaneously during the quasiperiodic *DP* 2 fluctuation events, if we allow for the temporal resolution of tens of seconds [*Kikuchi et al.*, 1996].

[26] *Kikuchi and Araki* [1979a] examined the one-dimensional transmission of the electric field in the ionospheric *E* region that was assumed to be a conductor with an anisotropic conductivity. The results showed that it took about one hour for the electric field to be transmitted to the equator if the daytime ionospheric condition was applied. The fast mode wave in the *F* region could play a role in the transmission of the polar electric field to the low latitude ionosphere, if the *F* region is assumed to be composed of fully ionized plasma. However, the ionospheric waveguide centered at the peak of the F2 layer allow the horizontal transmission of the fast mode MHD wave at frequencies above 1 Hz. The cutoff frequency never allows the transmission of the convection electric field to lower latitudes. *Strangeway and Raeder* [2001] also examined MHD waves in the partially ionized ionosphere, and pointed out that the collision-dominated ionosphere did not allow the Poynting flux to be transported horizontally. Furthermore, the fast mode in the *F* region suffers from attenuation due to the boundary condition at the conducting ionosphere [*Kikuchi and Araki*, 1979a]. Thus the electric field carried by the fast mode never plays a role in the horizontal transmission of the polar electric field to low latitudes.

[27] *Kikuchi et al.* [1978] and *Kikuchi and Araki* [1979b] suggested that the polar electric field could be transmitted to low latitudes by the zeroth-order TM mode in the Earth-ionosphere waveguide composed of the vacuum region bounded by the perfectly conducting ground and the semi-infinite conducting ionospheric *E* region with an anisotropic conductivity. The TM0 mode had no cutoff frequency and propagated at the speed of light, accompanying the electric currents in the conducting *E* region and on the surface of the ground. Since the TM0 mode has no cutoff frequency, both rapidly changing and quasi-steady electric fields can propagate to the equator. The propagating TM0 mode carries the Poynting flux in the space between the ground and the *E* region, accompanying electric currents in the *E* region. The Poynting flux of

the TM0 mode is composed of the transverse magnetic field and the vertical electric field that is deduced from the ionospheric electric potential with respect to the ground. In other words, the ionospheric potential given by FACs is transmitted instantaneously to low latitude by the TM0 mode in the waveguide.

[28] *Kikuchi and Araki* [1979b] also studied the propagation of the TM0 mode in a three-layer model composed of MHD medium (*F* region to magnetosphere), conductor (*E* region), and the vacuum region below the ionosphere. It was shown that the horizontal electric field deduced from the ionospheric current combined with the ionospheric conductivity was transported by Alfven waves upward along the magnetic field lines. The intensity of the upward transmitted electric field is determined as the ratio between the ionospheric current density and the conductivity, when the height-integrated ionospheric conductivity is much larger than the Alfvén conductance of the MHD medium [*Kikuchi and Araki*, 1979b]. Considering the geometry of the magnetic field lines, the electric field in the low-latitude *E* region will be transmitted to the equatorial *F* region, while the electric field is transmitted to the equatorial *E* region through the Earth-ionosphere waveguide. Consequently, the Earth-ionosphere waveguide model would be most promising to explain both the electric field in the *F* region and the electric currents in the *E* region, as observed with the Jicamarca radar and magnetometer at ANC, respectively.

[29] **Acknowledgments.** The authors thank the Canadian Space Agency for providing us with the CANOPUS magnetometer chain data and the Finnish Meteorological Institute for the International Monitor for Auroral Geomagnetic Effects magnetometer data. The LANL satellite energetic particle data were provided by G. Reeves of the Los Alamos National Laboratory. The authors wish to thank the Wind team and National Space Science Data Center for providing us with the solar wind parameters.

[30] Arthur Richmond thanks Christophe Peymirat and another reviewer for their assistance in evaluating this manuscript.

References

Araki, T., Global structure of geomagnetic sudden commencements, *Planet. Space Sci.*, *25*, 373–384, 1977.

Crooker, N. U., and G. L. Siscoe, Birkeland currents as the cause of the low-latitude asymmetric disturbance field, *J. Geophys. Res.*, *86*, 11,201–11,210, 1981.

Fejer, B. G., Low latitude electrodynamic plasma drifts: A review, *J. Atmos. Terr. Phys.*, *53*, 677–693, 1991.

Fejer, B. G., D. T. Farley, B. B. Balsley, and R. F. Woodman, Radar studies of anomalous velocity reversals in the equatorial ionosphere, *J. Geophys. Res.*, *81*, 4621–4626, 1976.

Fejer, B. G., C. A. Gonzales, D. T. Farley, M. C. Kelley, and R. F. Woodman, Equatorial electric fields during magnetically disturbed conditions: 1. The effect of the interplanetary magnetic field, *J. Geophys. Res.*, *84*, 5797–5802, 1979.

Gonzales, C. A., M. C. Kelley, B. G. Fejer, J. F. Vickrey, and R. F. Woodman, Equatorial electric fields during magnetically disturbed conditions: 2. Implications of simultaneous auroral and equatorial measurements, *J. Geophys. Res.*, *84*, 5803–5812, 1979.

Gonzales, C. A., M. C. Kelley, R. A. Behnke, J. F. Vickrey, R. Wand, and J. Holt, On the latitudinal variations of the ionospheric electric field during magnetospheric disturbances, *J. Geophys. Res.*, *88*, 9135–9144, 1983.

Gouin, P., Reversal of the magnetic daily variation at Addis Ababa, *Nature*, *193*, 1145–1146, 1962.

Hutton, R., and J. O. Oyinloye, The counter-electrojet in Nigeria, *Ann. Geophys.*, *26*, 921–926, 1970.

Iijima, T., Field-aligned currents in geospace: Substance and significance, in *Magnetospheric Current Systems*, *Geophys. Monogr. Ser.*, vol. 118, edited by S. Ohtani et al., pp. 107–129, AGU, Washington, D. C., 2000.

Iijima, T., and T. Nagata, Signatures for substorm development of the growth phase and expansion phase, *Planet. Space Sci.*, *20*, 1095–1112, 1972.

Iijima, T., and T. A. Potemra, The amplitude distribution of field-aligned currents at northern high latitudes observed by Triad, *J. Geophys. Res.*, *81*, 2165–2174, 1976.

Jaggi, R. K., and R. A. Wolf, Self-consistent calculation of the motion of a sheet of ions in the magnetosphere, *J. Geophys. Res.*, *78*, 2852–2866, 1973.

Kelley, M. C., B. G. Fejer, and C. A. Gonzales, An explanation for anomalous equatorial ionospheric electric fields associated with a northward turning of the interplanetary magnetic field, *Geophys. Res. Lett.*, *6*, 301–304, 1979.

Kikuchi, T., Evidence of transmission of polar electric fields to the low latitude at times of geomagnetic sudden commencements, *J. Geophys. Res.*, *91*, 3101–3105, 1986.

Kikuchi, T., and T. Araki, Transient response of uniform ionosphere and preliminary reverse impulse of geomagnetic storm sudden commencement, *J. Atmos. Terr. Phys.*, *41*, 917–925, 1979a.

Kikuchi, T., and T. Araki, Horizontal transmission of the polar electric field to the equator, *J. Atmos. Terr. Phys.*, *41*, 927–936, 1979b.

Kikuchi, T., T. Araki, H. Maeda, and K. Maekawa, Transmission of polar electric fields to the equator, *Nature*, *273*, 650–651, 1978.

Kikuchi, T., H. Lühr, T. Kitamura, O. Saka, and K. Schlegel, Direct penetration of the polar electric field to the equator during a *DP* 2 event as detected by the auroral and equatorial magnetometer chains and the EISCAT radar, *J. Geophys. Res.*, *101*, 17,161–17,173, 1996.

Kikuchi, T., M. Pinnock, A. Rodger, H. Lühr, T. Kitamura, H. Tachihara, M. Watanabe, N. Sato, and M. Ruohoniemi, Global evolution of a substorm-associated *DP* 2 current system observed by SuperDARN and magnetometers, *Adv. Space Res.*, *26*, 121–124, 2000a.

Kikuchi, T., H. Lühr, K. Schlegel, H. Tachihara, M. Shinohara, and T.-I. Kitamura, Penetration of auroral electric fields to the equator during a substorm, *J. Geophys. Res.*, *105*, 23,251–23,261, 2000b.

Kobea, A. T., C. Amory-Mazaudier, J. M. Do, H. Lühr, E. Hougninou, J. Vassal, E. Blanc, and J. J. Curto, Equatorial electrojet as part of the global circuit: A case-study from the IEEY, *Ann. Geophys.*, *16*, 698–710, 1998.

Kobea, A. T., A. D. Richmond, B. A. Emery, C. Peymirat, H. Lühr, T. Moretto, M. Hairston, and C. Amory-Mazaudier, Electrodynamic coupling of high and low latitudes: Observations on May 27, 1993, *J. Geophys. Res.*, *105*, 22,979–22,989, 2000.

Lyons, L. R., A new theory for magnetospheric substorms, *J. Geophys. Res.*, *100*, 19,069–19,081, 1995.

Nishida, A., Geomagnetic *DP* 2 fluctuations and associated magnetospheric phenomena, *J. Geophys. Res.*, *73*, 1795–1803, 1968a.

Nishida, A., Coherence of geomagnetic *DP* 2 fluctuations with interplanetary magnetic variations, *J. Geophys. Res.*, *73*, 5549–5559, 1968b.

Nishida, A., N. Iwasaki, and T. Nagata, The origin of fluctuations in the equatorial electrojet: A new type of geomagnetic variation, *Ann. Geophys.*, *22*, 478–484, 1966.

Onwumechilli, A., K. Kawasaki, and S.-I. Akasofu, Relationships between the equatorial electrojet and polar magnetic variations, *Planet. Space Sci.*, *21*, 1–16, 1973.

Peymirat, C., A. D. Richmond, B. A. Emery, and R. G. Roble, A magnetosphere-thermosphere-ionosphere electrodynamics general circulation model, *J. Geophys. Res.*, *103*, 17,467–17,477, 1998.

Peymirat, C., A. D. Richmond, and A. T. Kobea, Electrodynamic coupling of high and low latitudes: Simulations of shielding/overshielding effects, *J. Geophys. Res.*, *105*, 22,991–23,003, 2000.

Rastogi, R. G., Lunar effects in the counter-electrojet near the magnetic equator, *J. Atmos. Terr. Phys.*, *36*, 167–170, 1974.

Rastogi, R. G., Geomagnetic storms and electric fields in the equatorial ionosphere, *Nature*, *268*, 422–424, 1977.

Reddy, C. A., V. V. Somayajulu, and C. V. Devasia, Global scale electrodynamic coupling of the auroral and equatorial dynamo regions, *J. Atmos. Terr. Phys.*, *41*, 189–201, 1979.

Reddy, C. A., V. V. Somayajulu, and K. S. Viswanathan, Backscatter radar measurements of storm-time electric field changes in the equatorial electrojet, *J. Atmos. Terr. Phys.*, *43*, 817–827, 1981.

Rostoker, G., S.-I. Akasofu, J. Foster, R. A. Greenwald, Y. Kamide, K. Kawasaki, A. T. Y. Lui, R. L. McPherron, and C. T. Russell, Magnetospheric substorms: Definition and signatures, *J. Geophys. Res.*, *85*, 1663–1668, 1980.

Senior, C., and M. Blanc, On the control of magnetospheric convection by the spatial distribution of ionospheric conductivities, *J. Geophys. Res.*, *89*, 261–284, 1984.

Sergeev, V. A., N. P. Dmitrieva, and E. S. Barkova, Triggering of substorm expansion by the IMF directional discontinuities: Time delay analysis, *Planet. Space Sci.*, *34*, 1109–1118, 1986.

Somayajulu, V. V., C. A. Reddy, and K. S. Viswanathan, Penetration of magnetospheric convective electric field to the equatorial ionosphere during the substorm of March 22, 1979, *Geophys. Res. Lett.*, *14*, 876–879, 1987.

Somayajulu, V. V., L. Cherian, K. Rajeev, G. Ramkumar, and C. R. Reddi, Mean winds and tidal components during counter electrojet events, *Geophys. Res. Lett.*, *20*, 1443–1446, 1993.

Spiro, R. W., R. A. Wolf, and B. G. Fejer, Penetration of high-latitude-electric-field effects to low latitudes during SUNDIAL 1984, *Ann. Geophys.*, *6*, 39–50, 1988.

Strangeway, R. J., and J. Raeder, On the transition from collisionless to collisional magnetohydrodynamics, *J. Geophys. Res.*, *106*, 1955–1960, 2001.

Tanaka, T., Generation mechanisms for magnetosphere-ionosphere current systems deduced from a three-dimensional MHD simulation of the solar wind-magnetosphere-ionosphere coupling processes, *J. Geophys. Res.*, *100*, 12,057–12,074, 1995.

Tsunomura, S., and T. Araki, Numerical analysis of equatorial enhancement of geomagnetic sudden commencement, *Planet. Space Sci.*, *32*, 599–604, 1984.

Vasyliunas, V. M., The interrelationship of magnetospheric processes, in *Earth's Magnetospheric Processes*, edited by B. M. McCormac, pp. 29–38, D. Reidel, Norwell, Mass., 1972.

B. Fejer, Utah State University, Center for Atmospheric and Space Sciences, 246 SER Building, 4405 Old Main Building, Logan, UT 84322-4405, USA. (bfejer@cc.usu.edu)

K. K. Hashimoto and T. Kikuchi, Communications Research Laboratory, Applied Research and Standard Division, 4-2-1 Nukui-Kitamachi, Koganei, Tokyo, 184-8795, Japan. (hashimoto@crl.go.jp; kikuchi@crl.go.jp)

T.-I. Kitamura and H. Tachihara, Department of Earth and Planetary Sciences, Kyushu University, 33 Hakozaki, Fukuoka 812-81, Japan.